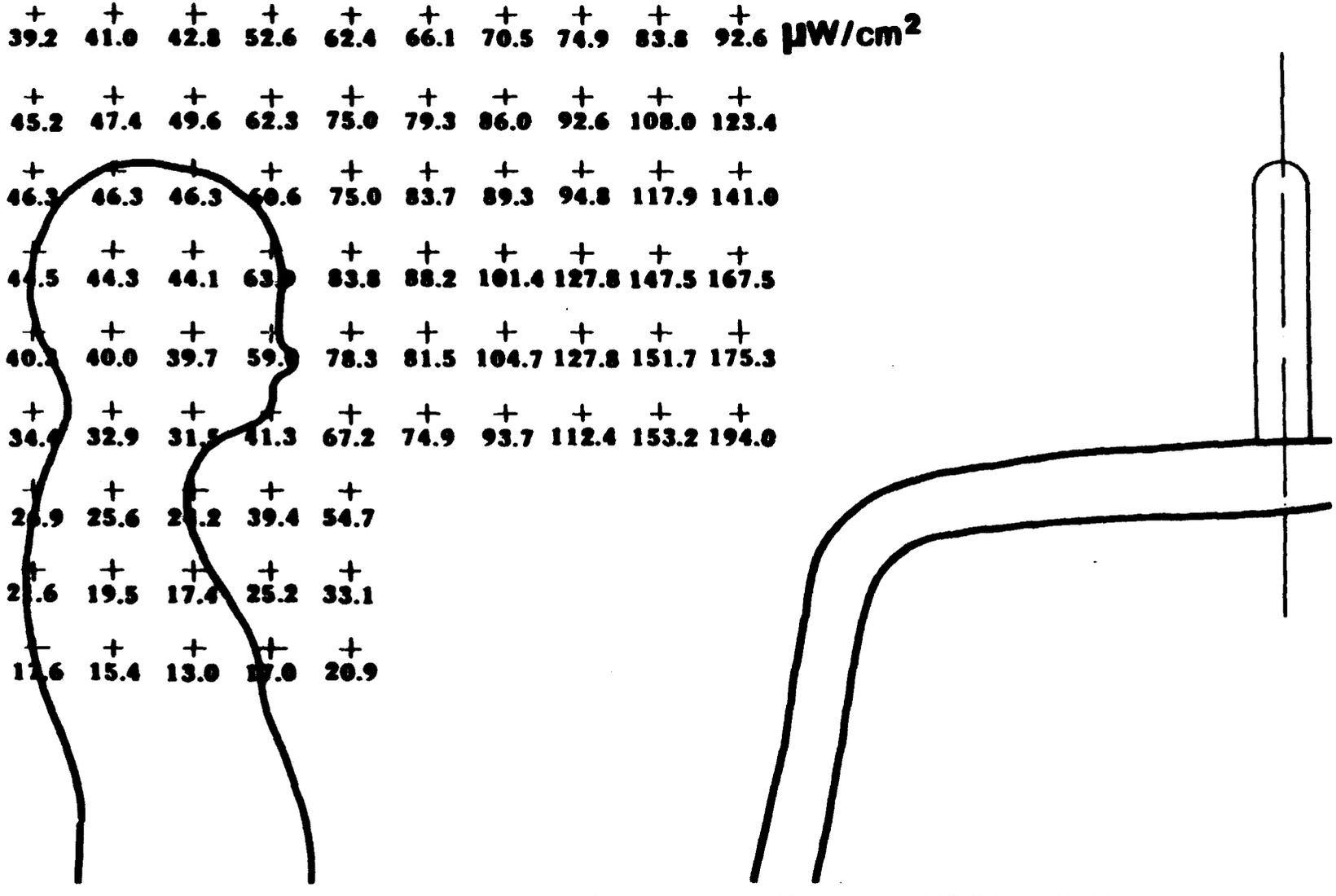

Fig. 37. Power densities exterior of automobile due to 835-MHz radiation from roof-mounted antenna, with 1-W input power (outline shows position of exposed child model held 63 cm from antenna).

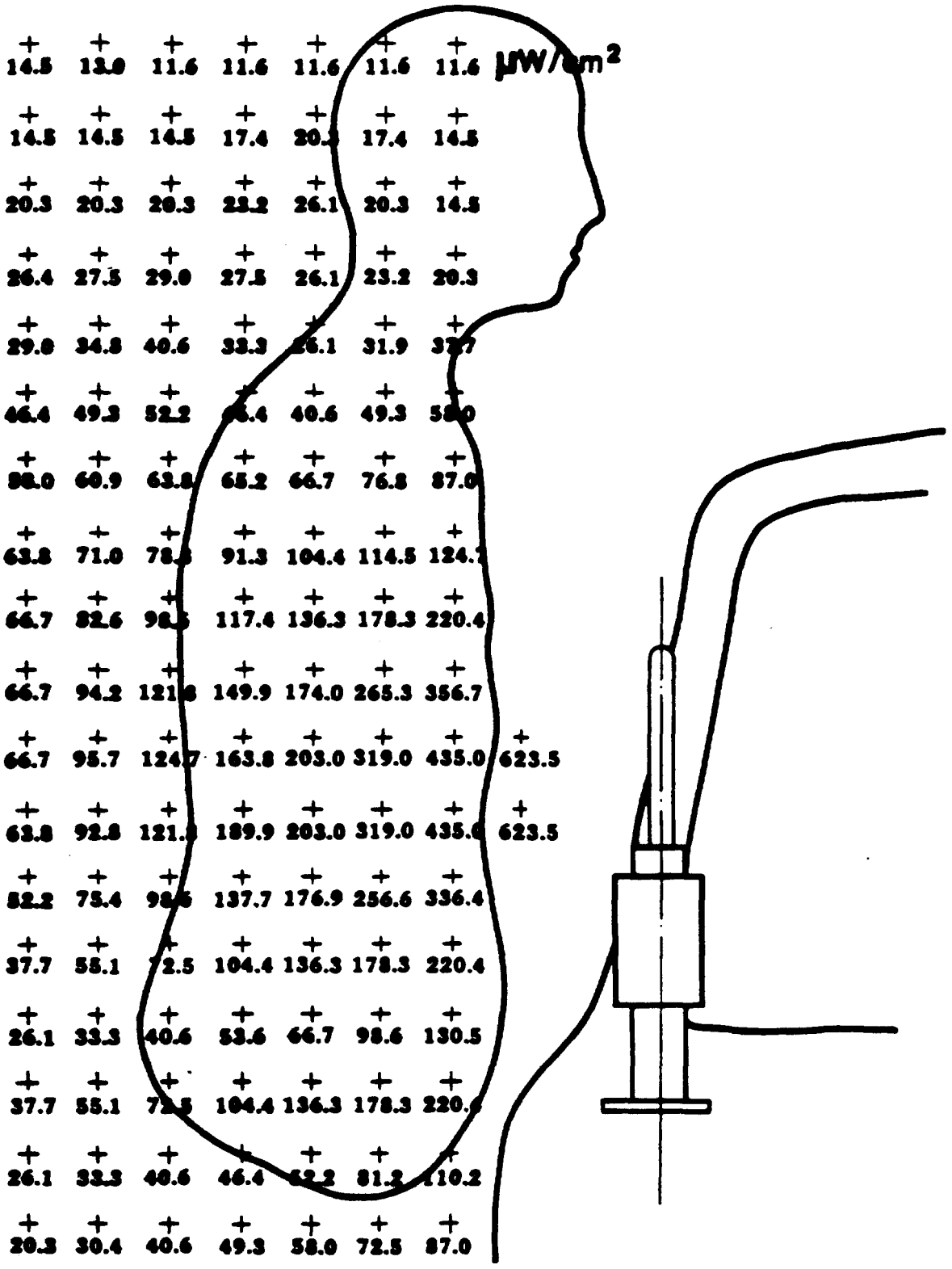

Fig. 38. Power densities exterior of automobile due to 835-MHz radiation from trunk-mounted antenna, with 1-W input power (outline shows position of exposed man model standing 12 cm from antenna).

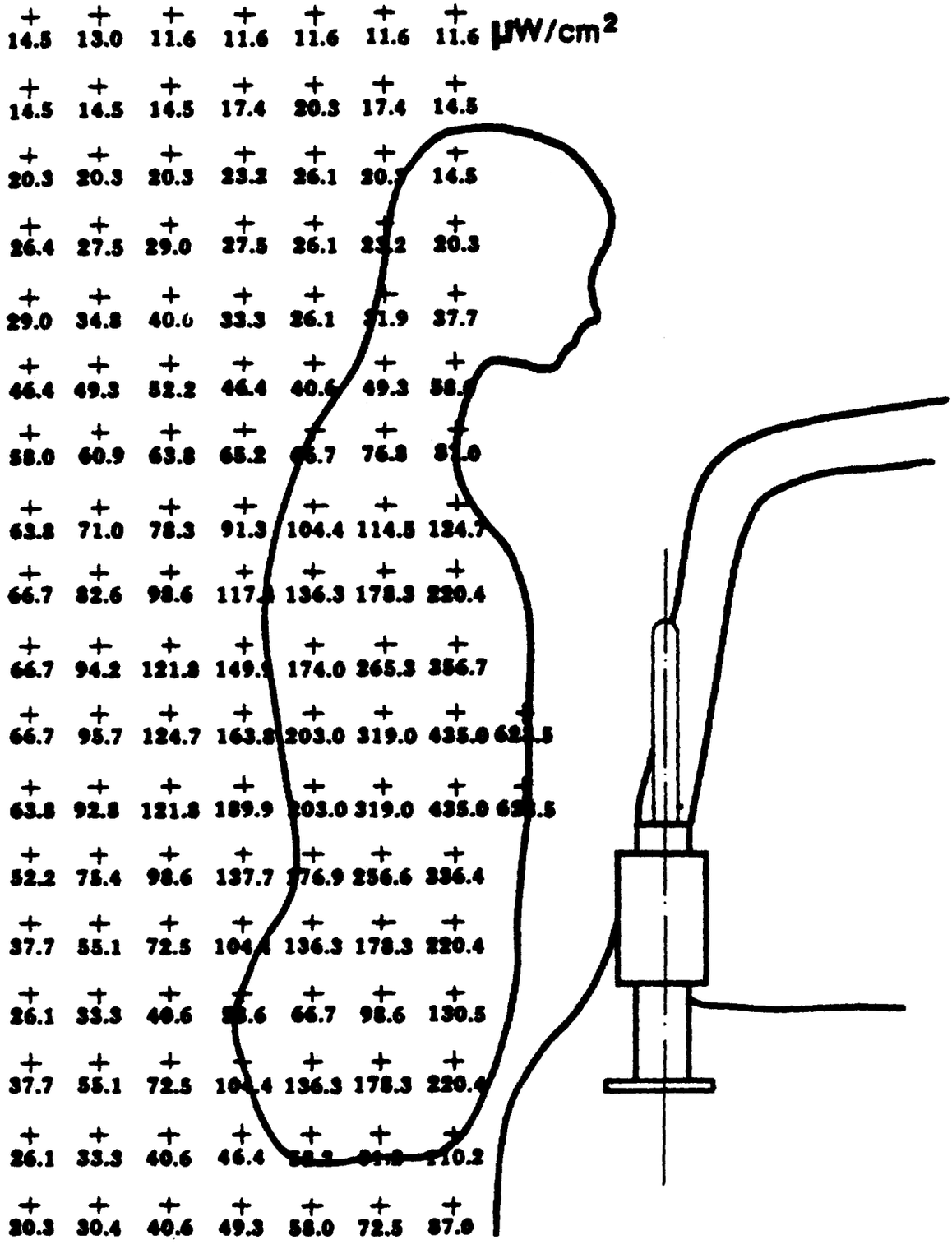

Fig. 39. Power densities exterior of automobile due to 835-MHz radiation from trunk-mounted antenna with 1-W input power (outline shows position of exposed woman model standing 9.7 cm from antenna).

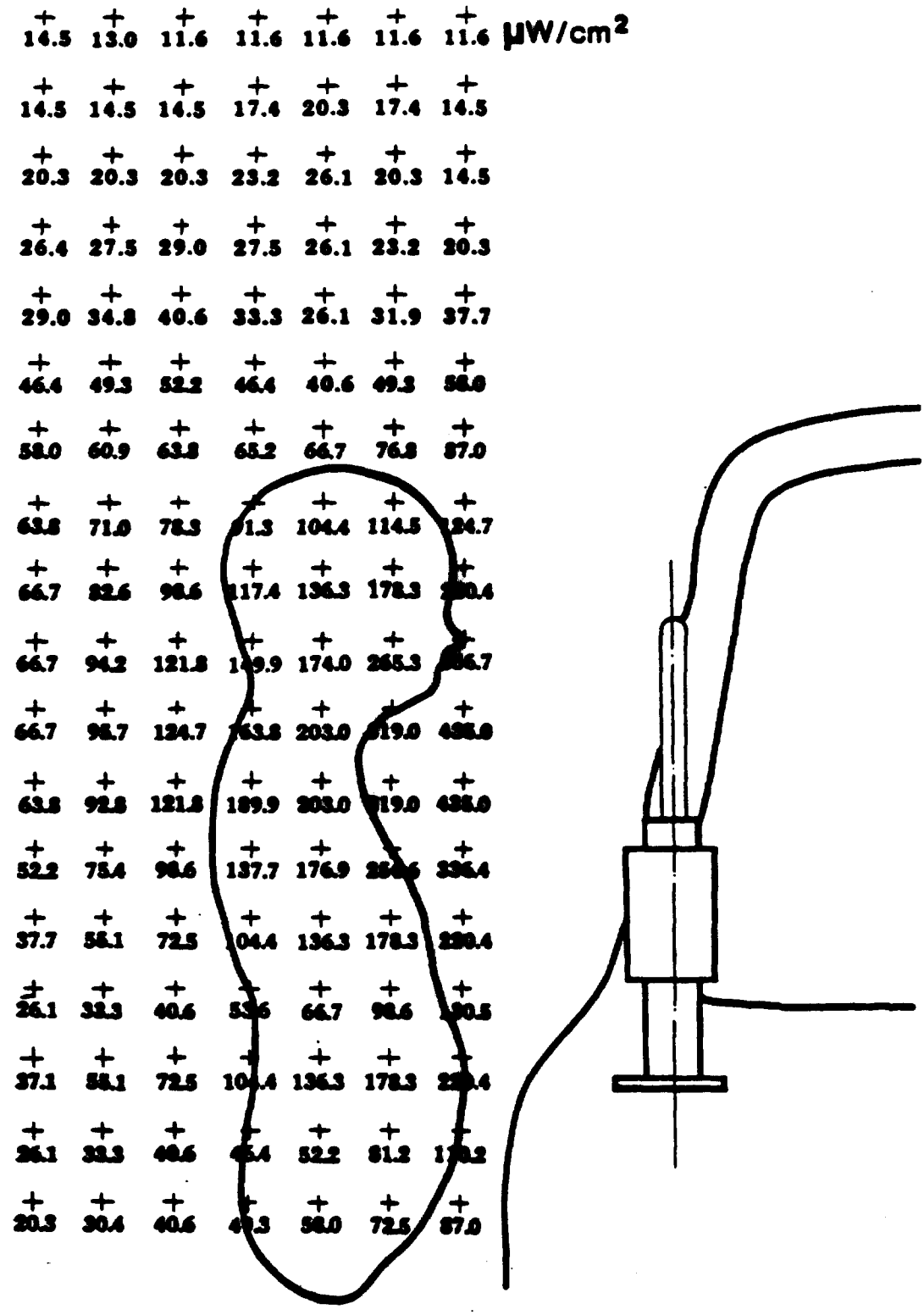

Fig. 40. Power densities exterior of automobile due to 835-MHz radiation from trunk-mounted antenna with 1-W input power (outline shows position of exposed child model standing 15 cm from antenna).

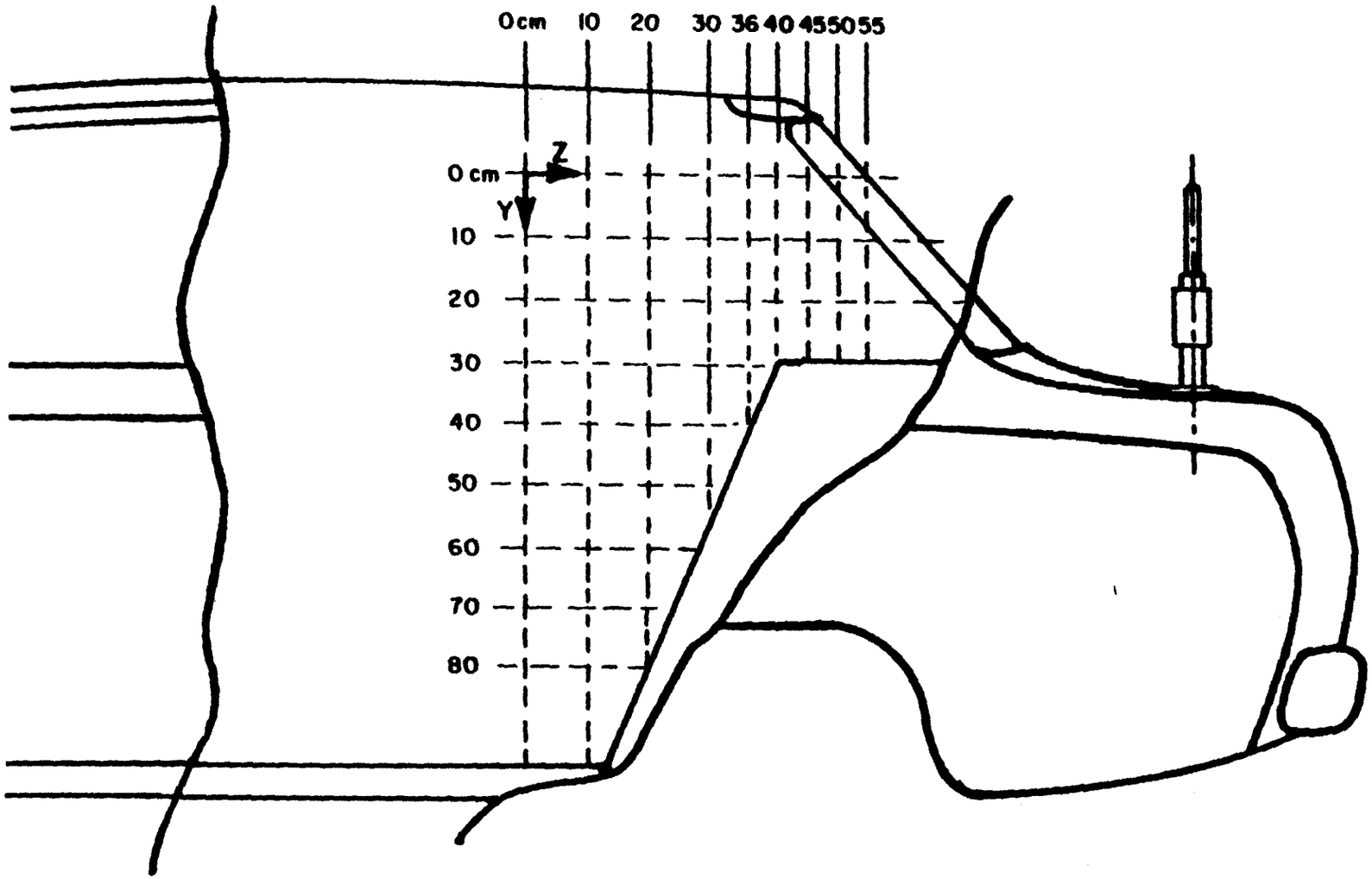

Fig. 41. Region in autombile (Y-Z plane) where power densities due to 835-MHz radiation from trunk-mounted antenna were measured (each intersection of dashed lines corresponds to measurement point).

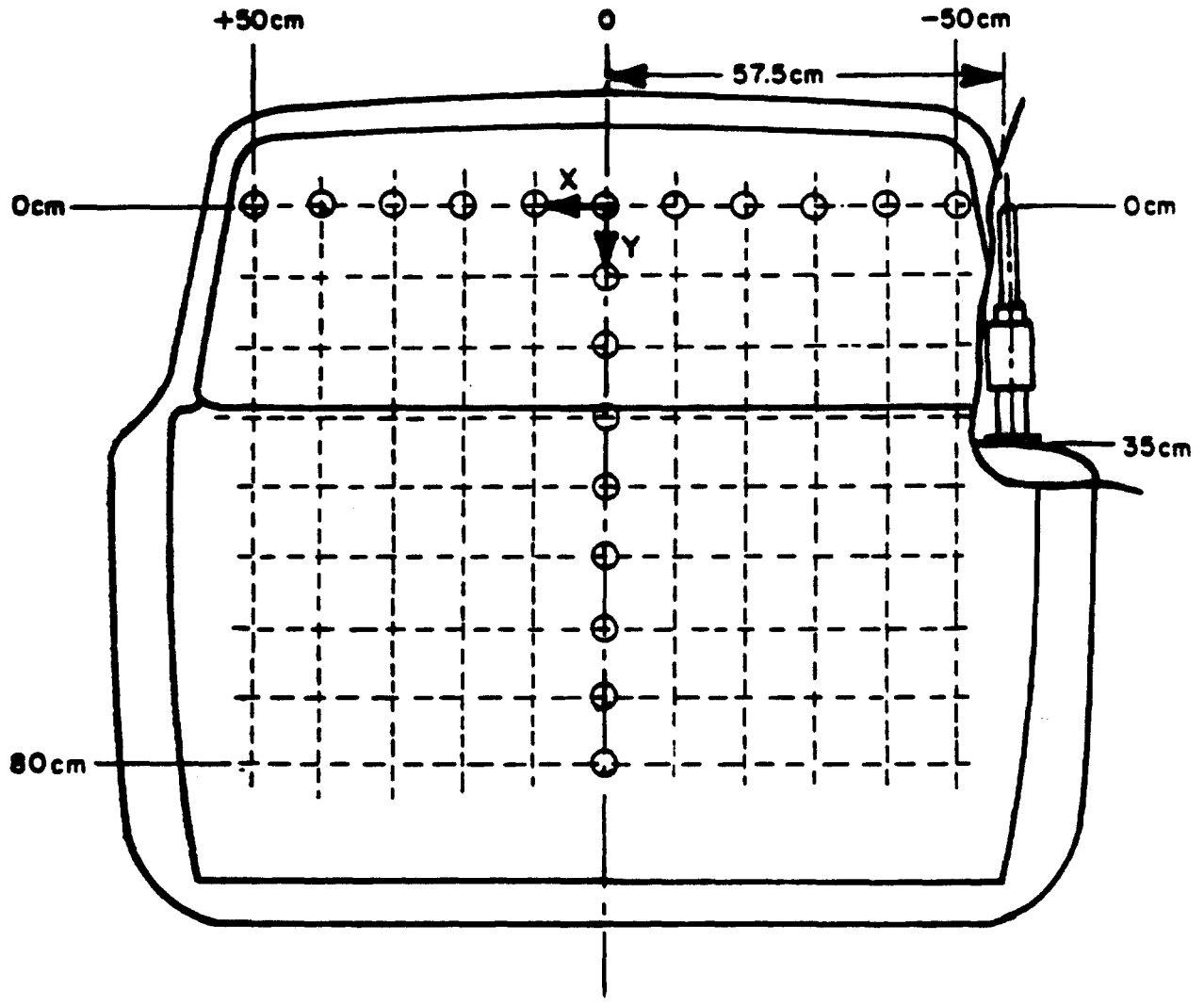

Fig. 42. Region in automobile (X-Y plane) where power densities due to 835-MHz radiation from trunk-mounted antenna were measured (each intersection of dashed lines corresponds to measurement point).

the automobile are shown in Figs. 43 through 46. The outline of the subjects are superimposed on the values of power density measured without the presence of the subjects.

Thermography

Exposure of Subjects to Roof-Mounted Antenna

The thermograph scans for the exposures of the adult woman standing 43.5 and 63 cm from the roof-mounted antenna are shown in Figs. 47-50. Thermograms were taken of sagittal scans through the head and also of horizontal scans through the eye region. The intensity scan (brightness proportional to temperature or SAR) is shown in the upper left of each figure. A profile scan with multiple scans with vertical deflections proportional to temperature or SAR is shown in the upper right of each figure. The lower three thermograms illustrated in each figure consist of a B-scan taken before exposure and a B-scan after exposure along the lines A-A', B-B', C-C' as noted on the intensity scan. The exposure time for these models was approximately 60 sec. We determined the maximum SAR by noting the maximum temperature differences before and after exposure obtained from the double B-scans and based on the specific heat and density of the phantom tissue given in Table 2. The maximum SAR levels were calculated. Since the SAR is proportional to the temperature differences denoted by the B-scans, one can easily visualize the SAR distribution from the vertical distance between these scans.

For the 63-cm-distance exposures the model was erect, whereas for the 43.5 cm exposures the model was leaning toward the antenna at the closest possible distance. The maximum SARs of 48.9 mW/kg per watt for the leaning woman model and 22.7 mW/kg per watt for the standing woman model occurred at the nose, as expected since it is the closest point of the body to the radiating antenna and it consists of wedge-shaped tissue, which allows greater energy penetration. Significant absorption was also found in the forehead, mouth, eye, temple, and neck. Based on the exposure

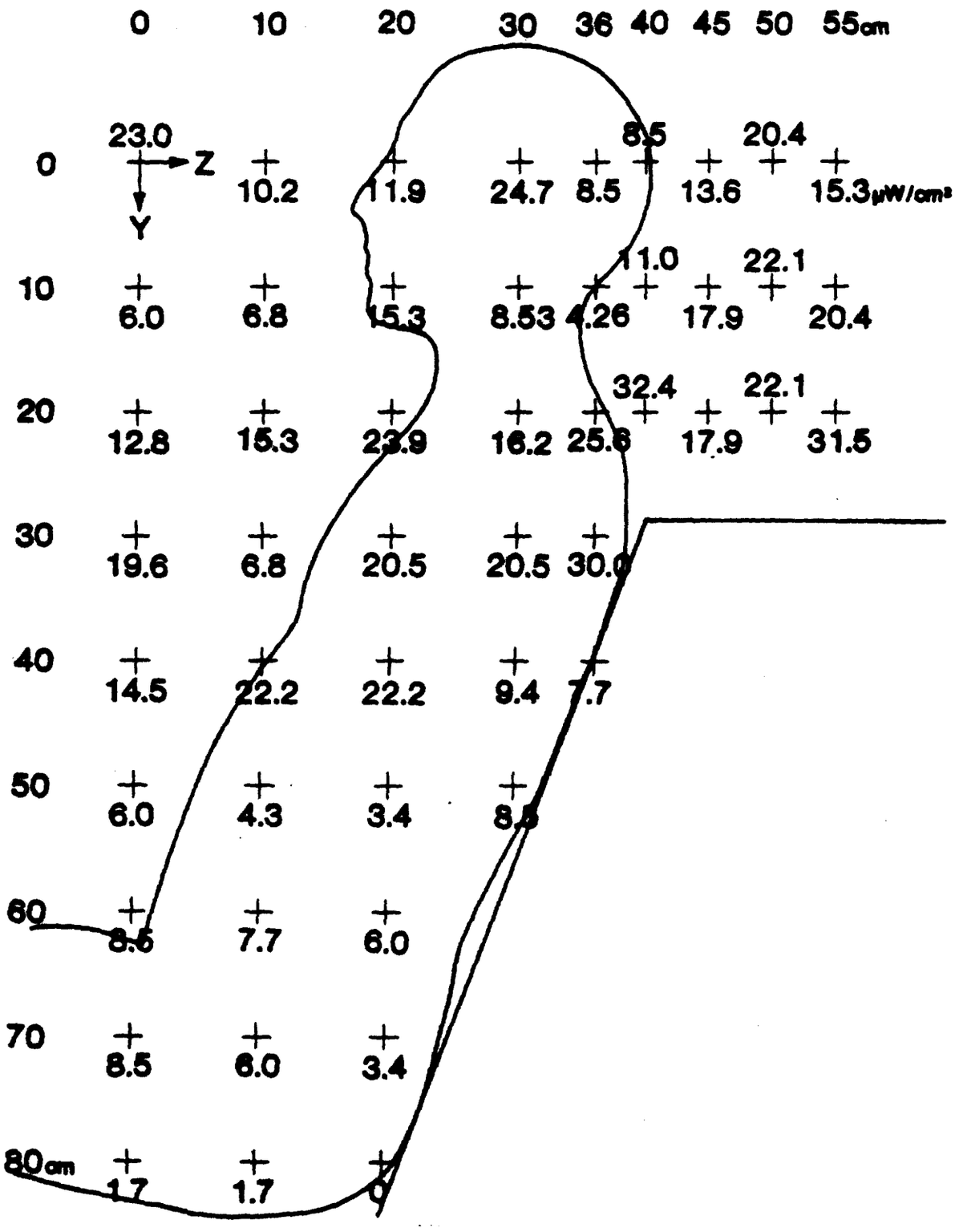

Fig. 43. Position of sitting man model interior of automobile exposed to 835-MHz radiation from trunk-mounted antenna with 1-W input power (Y-Z plane, X= 30cm).

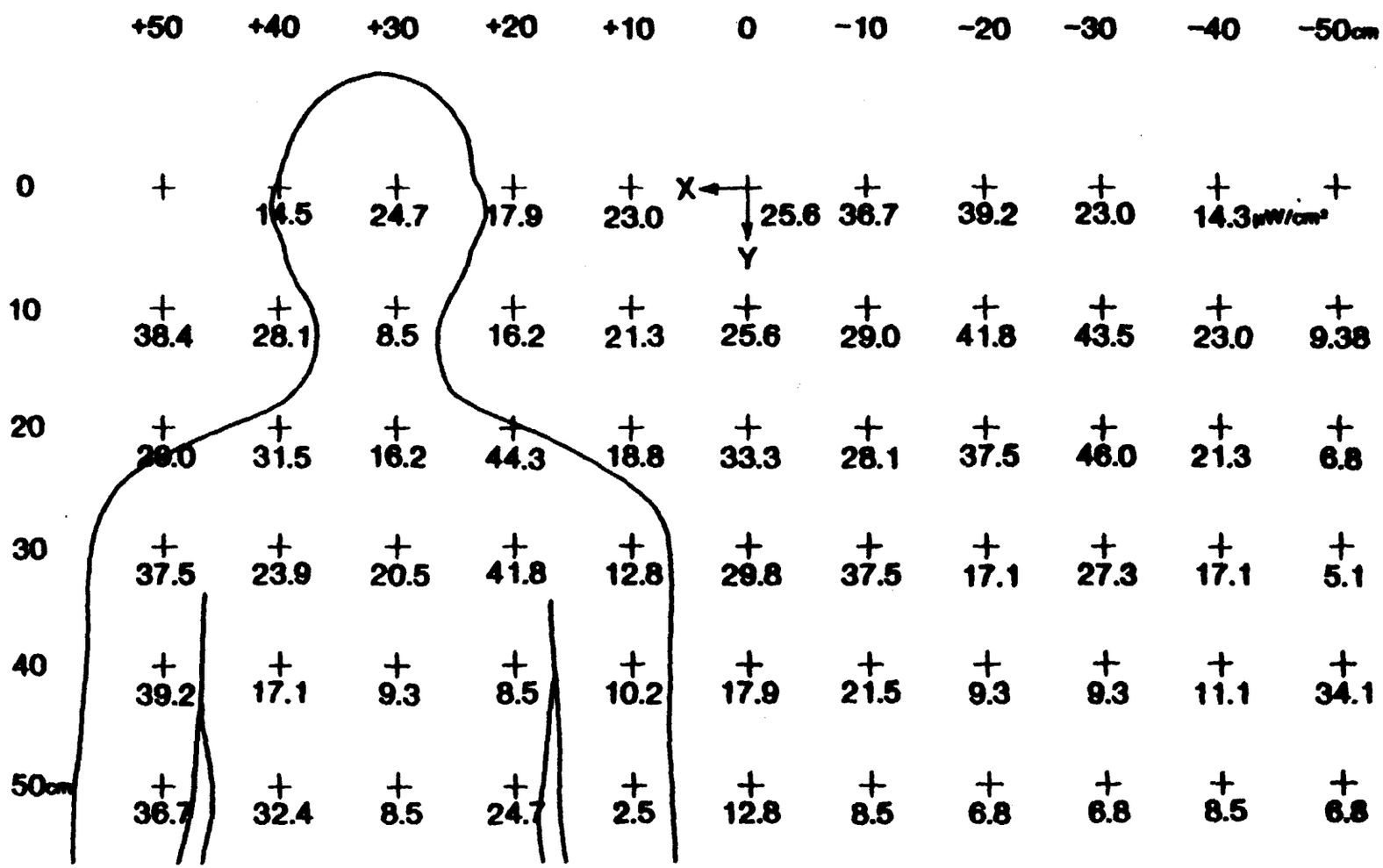

Fig. 44. Position of sitting man model interior of automobile exposed to 835-MHz radiation from trunk-mounted antenna with 1-W input power (X-Y plane, Z= 30 cm).

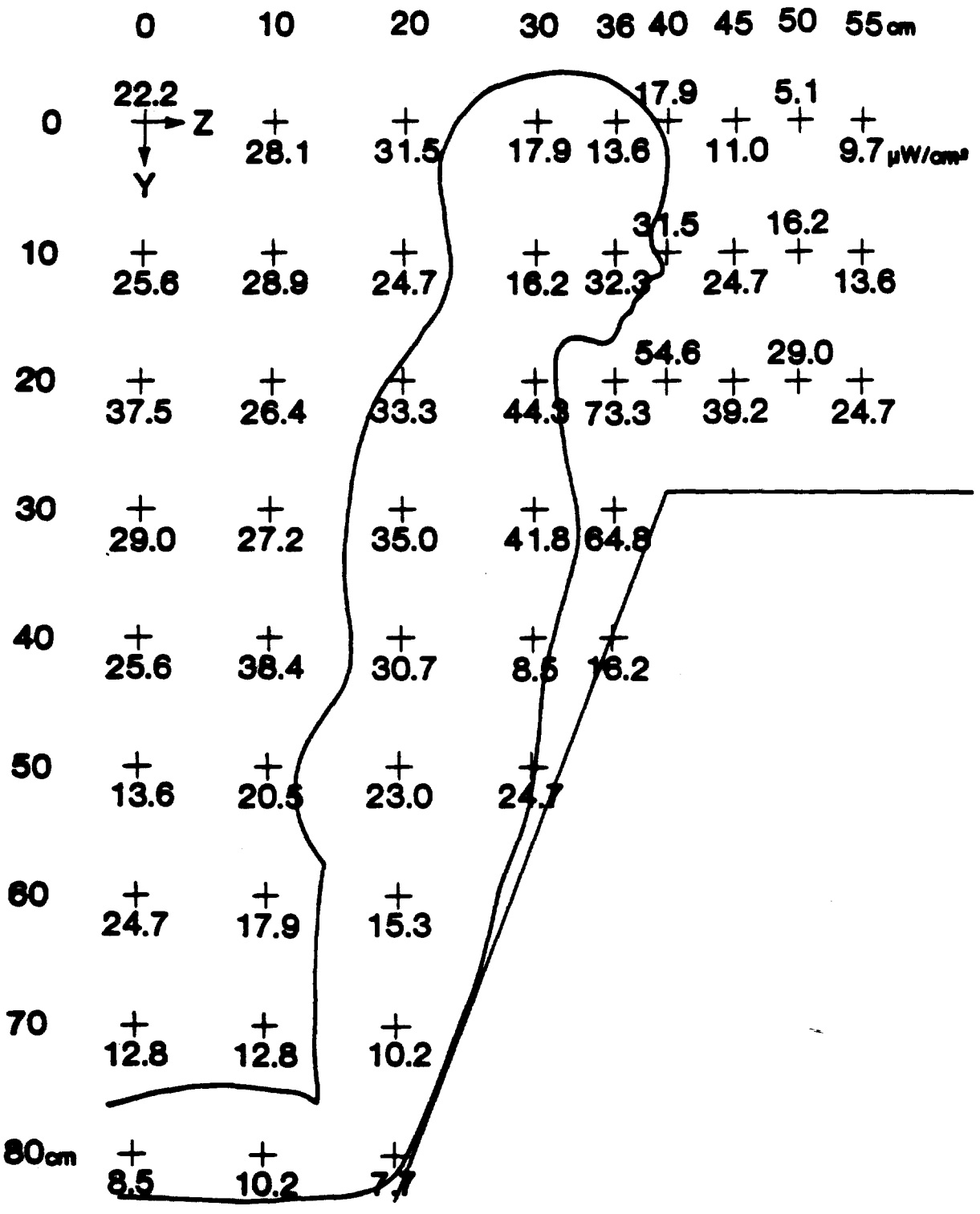

Fig. 45. Position of kneeling child model interior of automobile exposed to 835-MHz radiation from trunk-mounted antenna with 1-W input power (Y-Z plane, X= 20 cm).

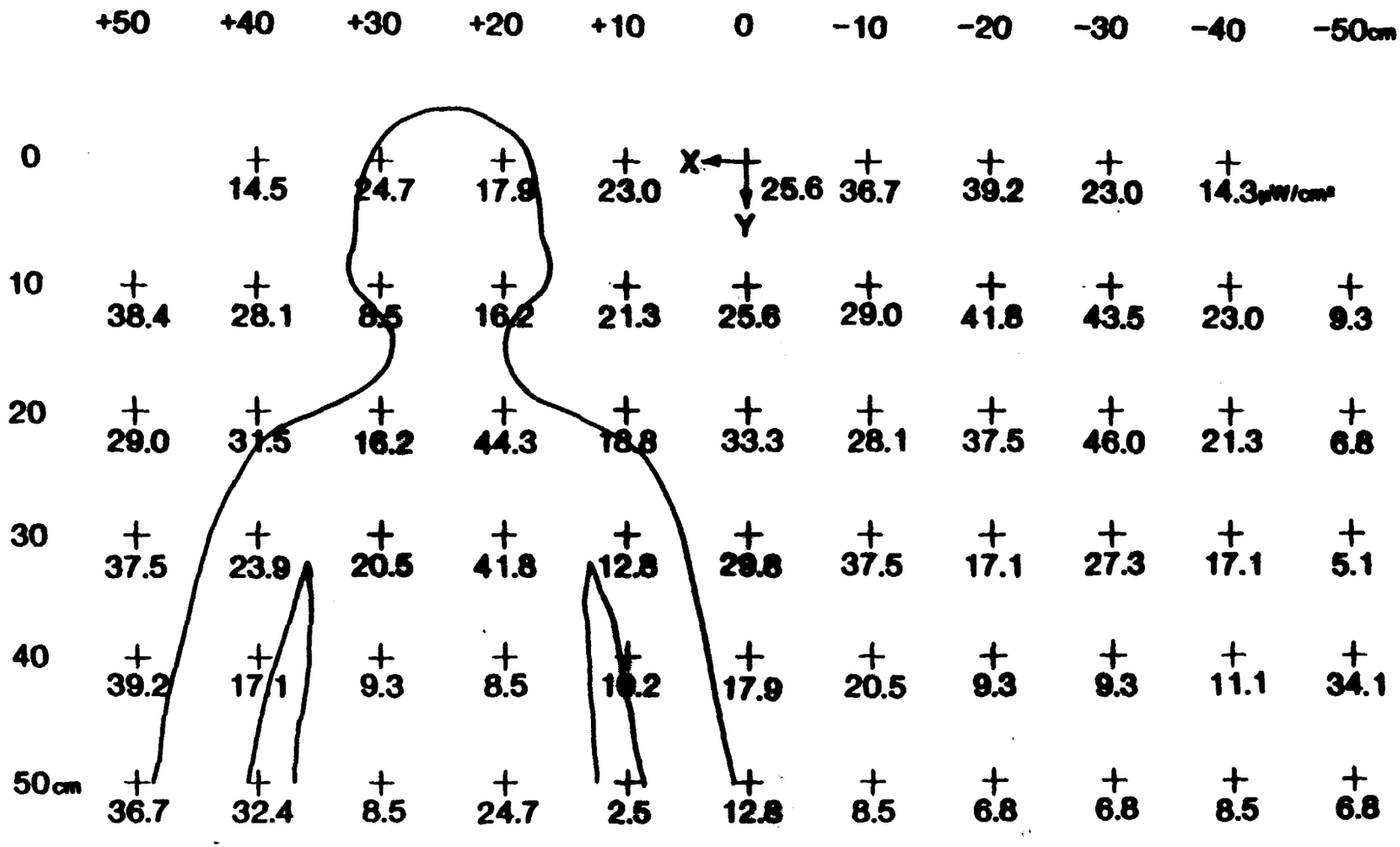

Fig. 46. Position of kneeling child model interior of automobile exposed to 835-MHz radiation from trunk-mounted antenna with 1-W input power (X-Y plane, Z= 30 cm).

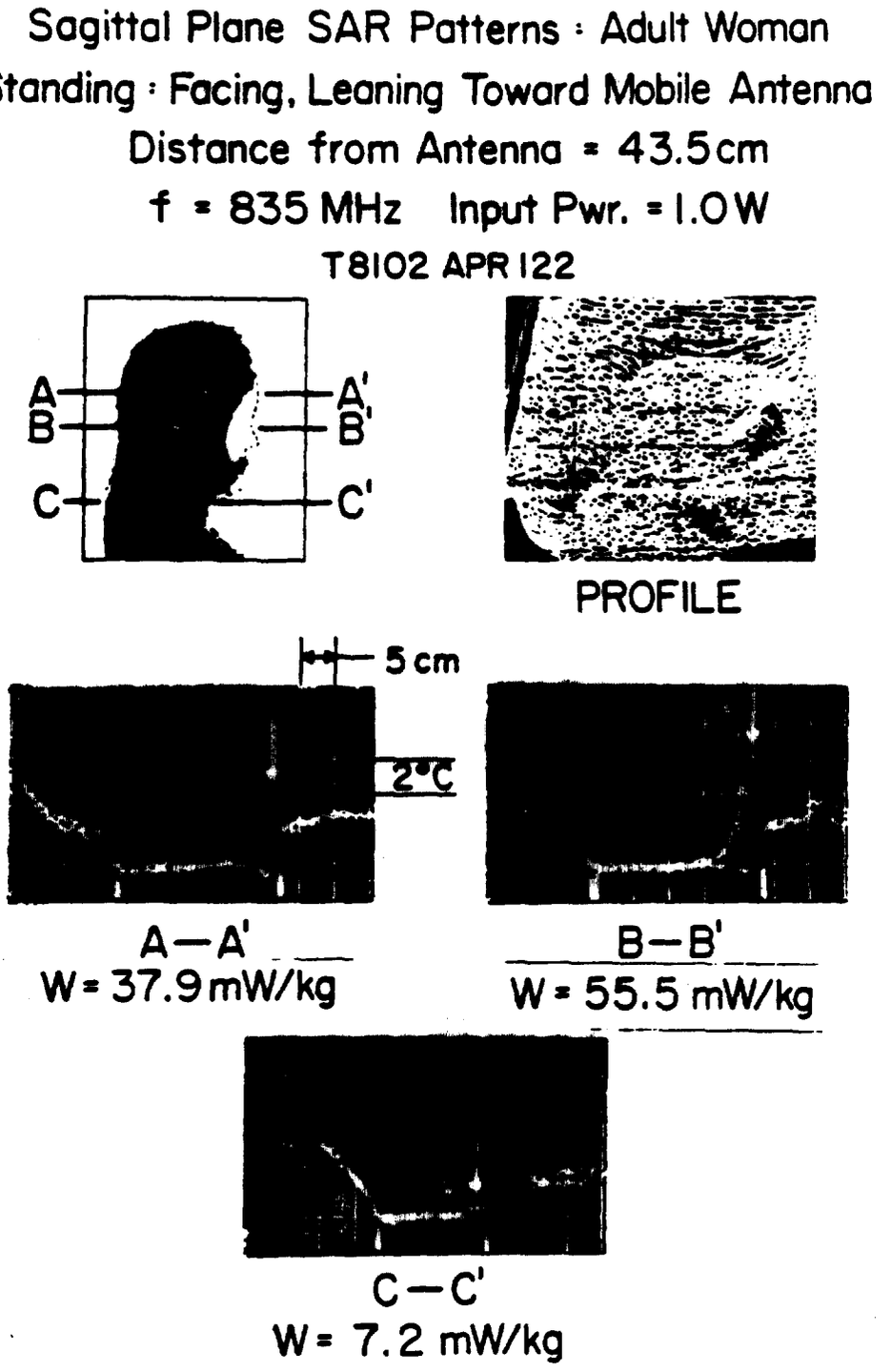

Fig. 47. Thermographically measured SAR patterns in woman model exposed 43.5 cm from roof-mounted antenna (sagittal plane).

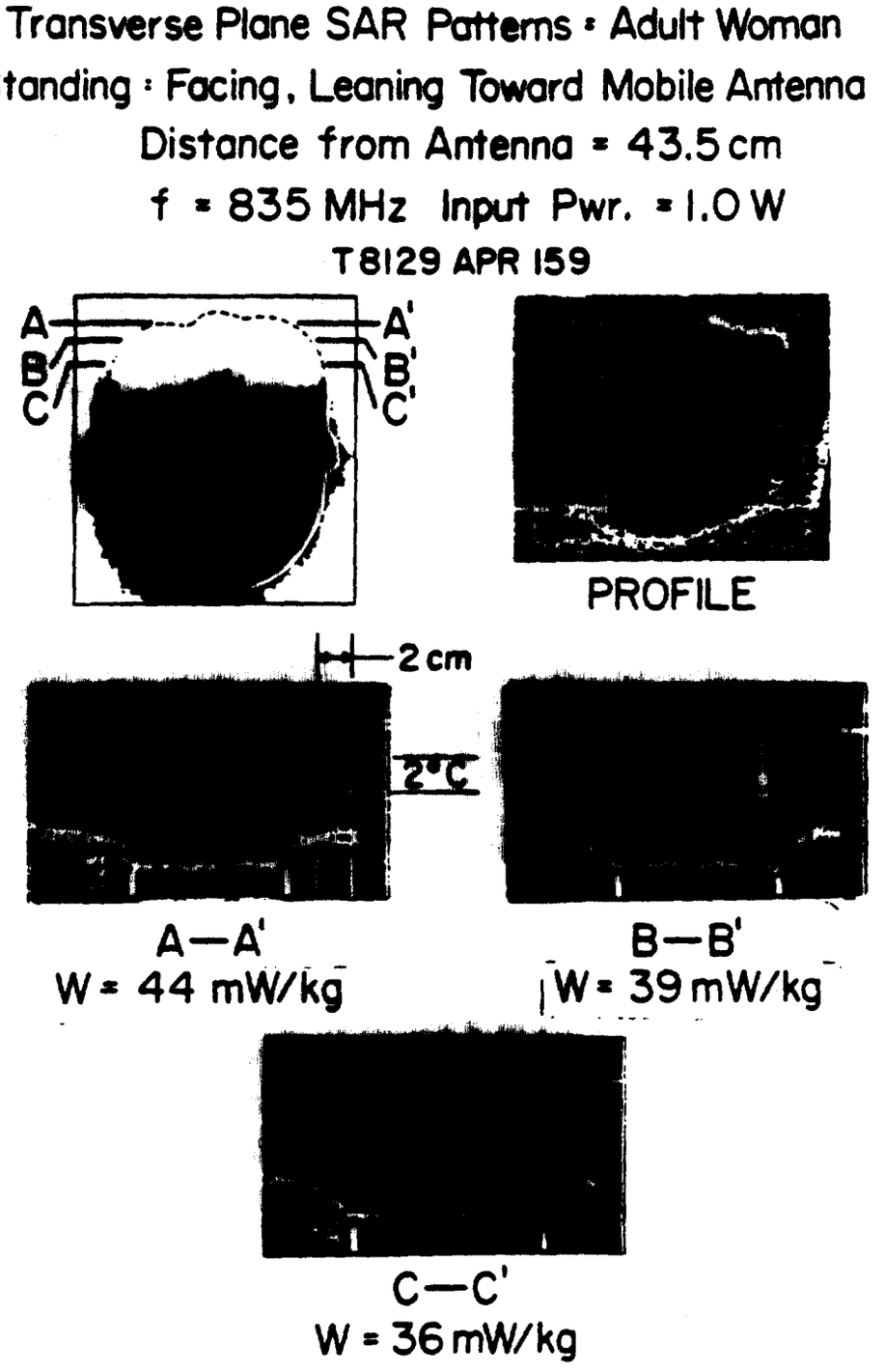

Fig. 48. Thermographically measured SAR patterns in woman model exposed 43.5 cm from roof-mounted antenna (transverse plane through eyes).

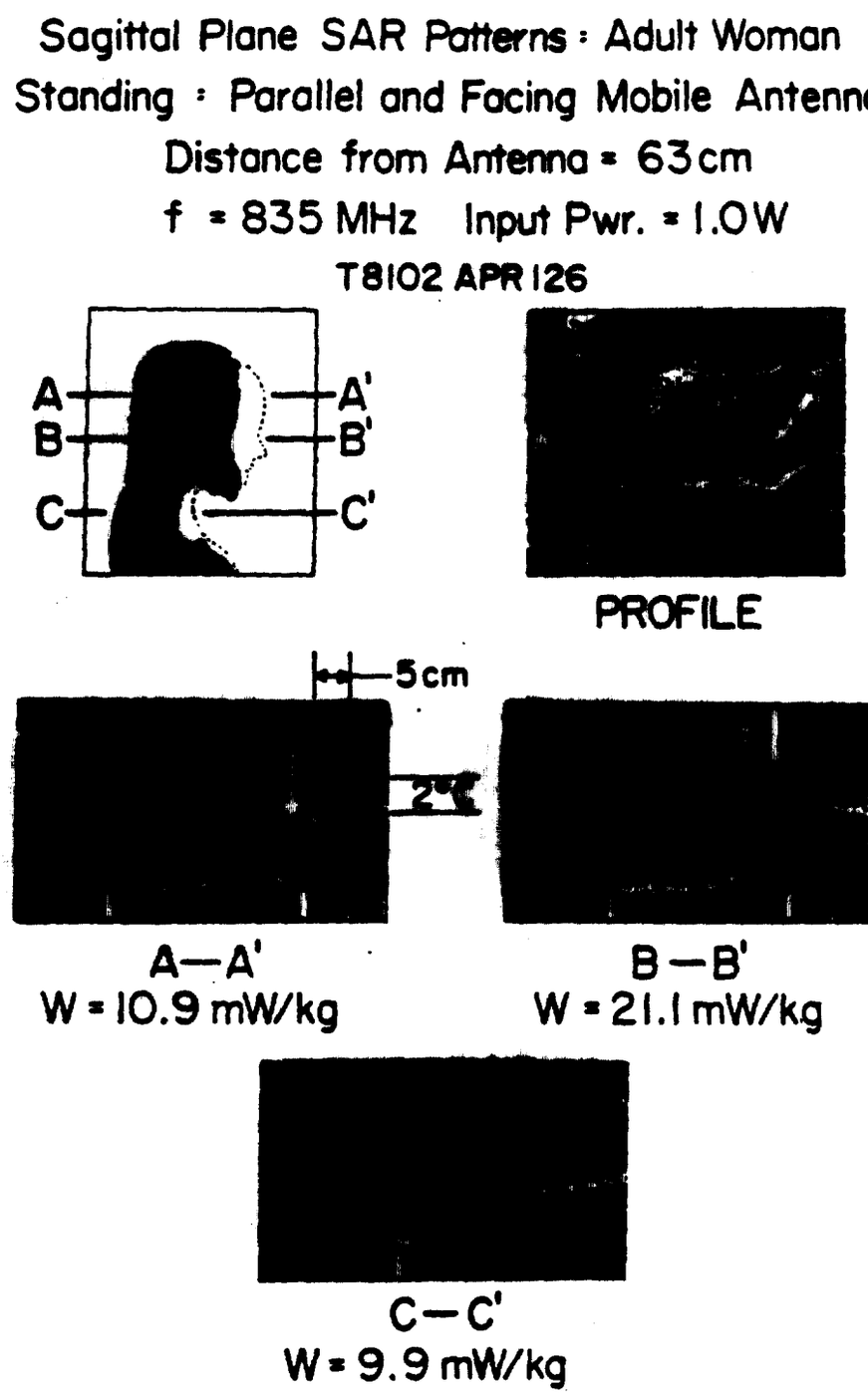

Fig. 49. Thermographically measured SAR patterns in woman model exposed 63 cm from roof-mounted antenna (sagittal plane).

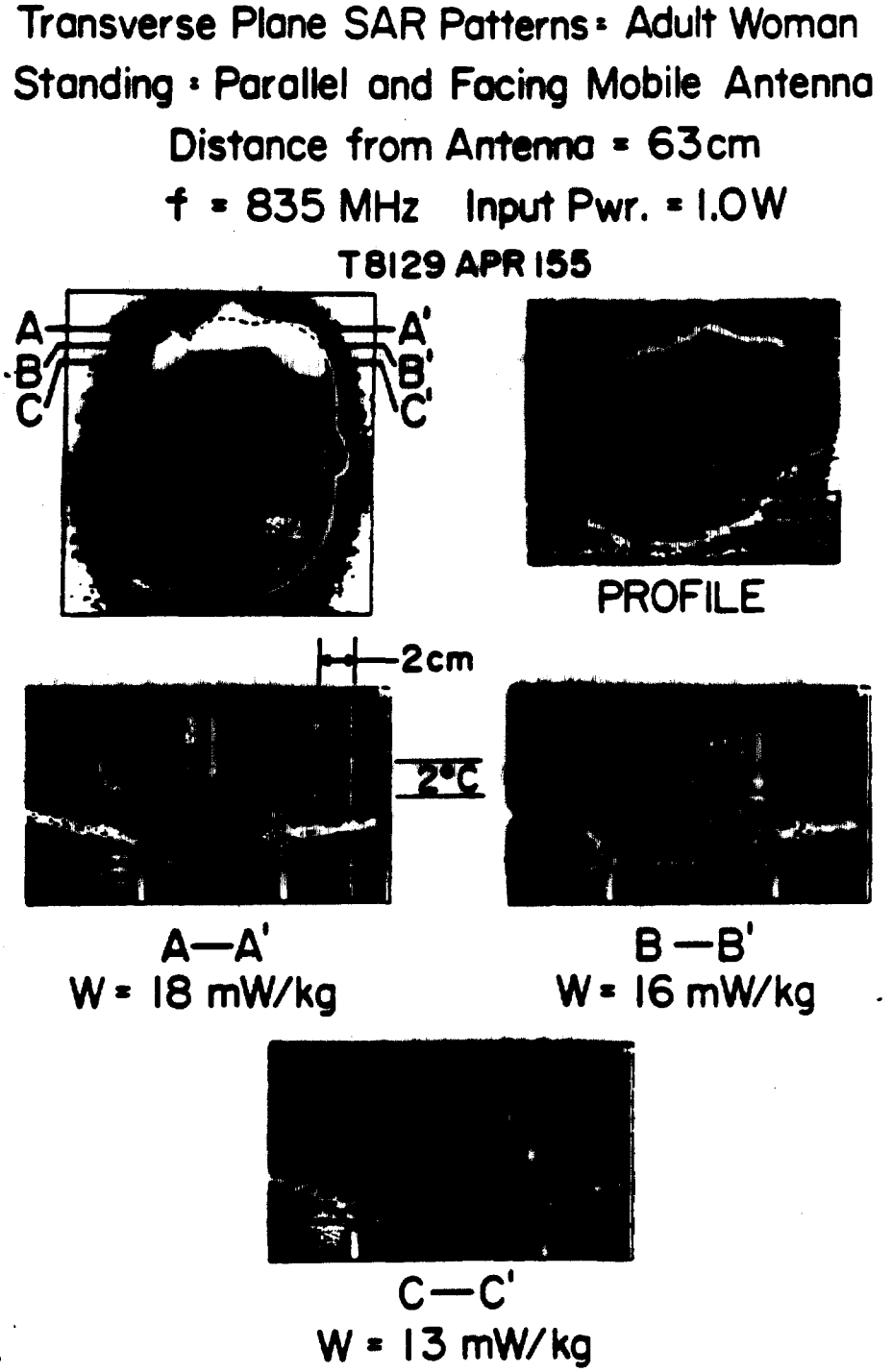

Fig. 50. Thermographically measured SAR patterns in woman model exposed 63 cm from roof-mounted antenna (transverse plane).

levels given in Figs. 34 to 37, the maximum SAR varied from .3 to .44 W/kg per mW/cm^2 incident to the subject.

In Figs. 51-54 are illustrated the thermograms taken for the child model exposed to the roof-mounted antenna. For this series the child was oriented 39 and 63 cm from the radiating antenna. At 39 cm, the child was assumed to be held by an adult as closely as possible to the antenna. Thermograms were taken for both the sagittal plane and the transverse plane cut through the orbital area of the child. The patterns for the child were similar to those of the woman, with maximum SAR levels reaching as high as 51.7 mW/kg-per-watt input into the antenna or .35 W/kg per mW/cm^2 incident to the head of the child. In Table 5 are summarized the maximum SARs in mW/kg per watt input for both the child and the adult woman model exposed to the roof-mounted antenna for different regions of the body.

Exposure of Subjects to Trunk-Mounted Mobile Antenna

All thermography relating to the exposures of the models to the trunk-mounted antenna were recorded digitally and analyzed by the computer methodology discussed in Appendix A. In Fig. 55 are illustrated the thermograms taken for the standing man exposed with the abdomen 12 cm from the trunk-mounted antenna. The figure at the upper-left-hand corner of the Fig. 55 is a profile scan in which the horizontal scale corresponds to horizontal position and the left-hand scale corresponds to the vertical position. The vertical deflection of each scan is proportional to SAR with the values given by the SAR scale at the right of the figure. The display at the upper-right-hand corner of the figure is an intensity scan in which the darkness is proportional to the SAR. The outline of the man is superimposed on the intensity scan. Single horizontal scans of SAR are shown at the lower half of the figure corresponding to the scan lines given in the upper right of the figure. The deflection at the bottom of the upper left scan is an artifact due to a hot spot outside of the section of the displayed thermograph frame.

TABLE 5. a) SARs IN WOMAN MODEL EXPOSED TO ROOF-MOUNTED ANTENNA (mW/kg PER WATT)

		Eyes	Nose	Temple	
Horizontal plane at eye level	Standing straight (63 cm)	15.0 ± 0.8	17.0 ± 0.8	13	
	Leaning forward (43.5 cm)	38.0 ± 1.4	42.7 ± 1.9	36	
		Forehead	Nose	Mouth	Neck
Sagittal plane	Standing straight (63 cm)	11.5 ± 1.7	22.7 ± 1.3	13.7 ± 1.8	9.3 ± 1.2
	Leaning forward (43.5 cm)	14.4 ± 3.2	48.9 ± 9.4	28 ± 4.2	8.1 ± 1.3

TABLE 5. b) SARs IN CHILD MODEL EXPOSED TO ROOF-MOUNTED ANTENNA (mW/kg PER WATT)

		Eyes	Nose	Temple	
Horizontal plane at eye level	Standing straight (63 cm)	19.4 ± 2.6	17.4 ± 2.6	13.4 ± 0.5	
	Leaning forward (39 cm)	31.3 ± 2.7	36.0 ± 0.2	19.1 ± 3.5	
		Forehead	Nose	Mouth	Neck
Sagittal plane	Standing straight (63 cm)	5.8 ± 1.5	10.2 ± 1.7	4.0 ± 1.3	15.2 ± 1.9
	Leaning forward (39 cm)	21.6	51.7	16.1	27.5

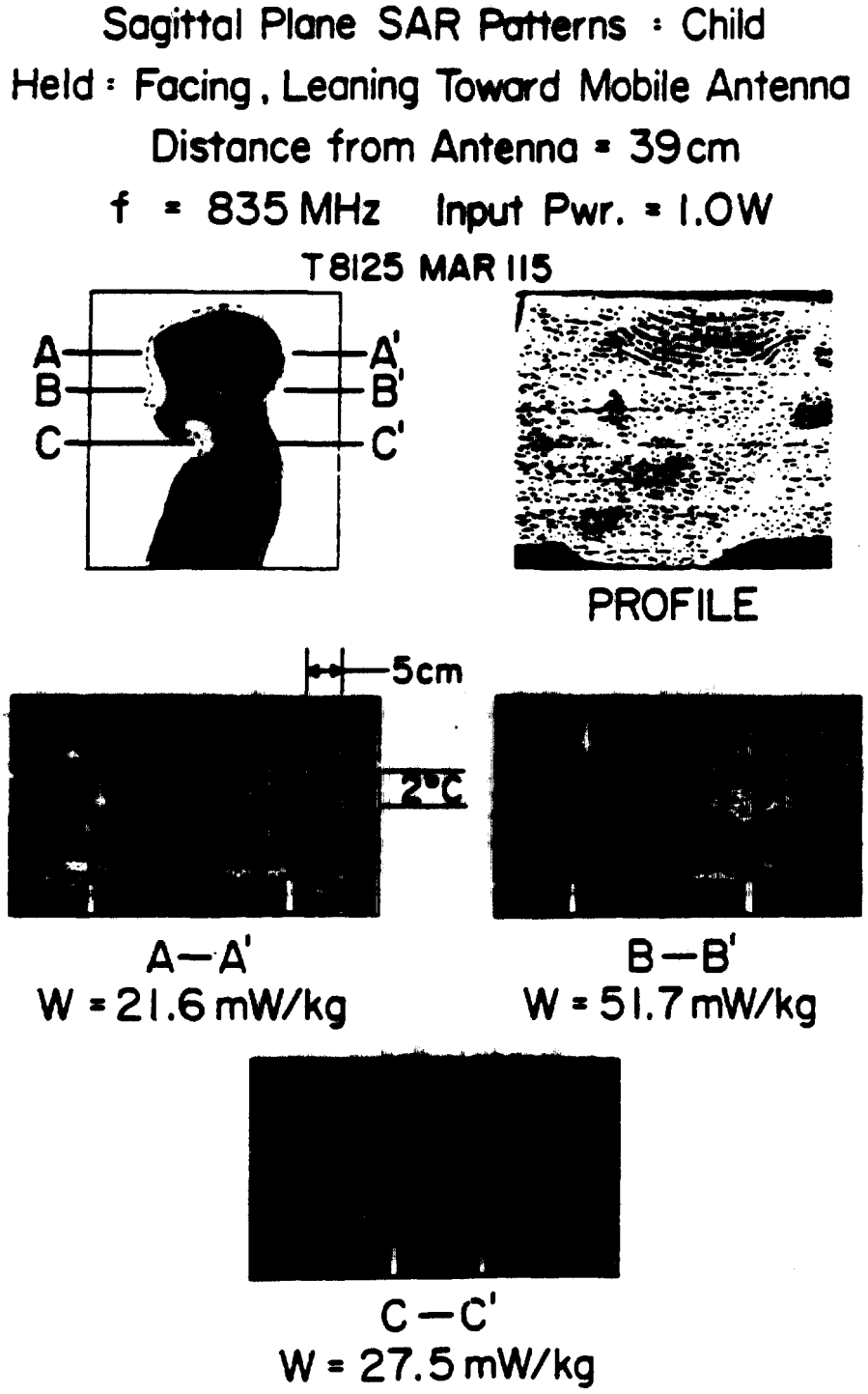

Fig. 51. Thermographically measured SAR patterns in child model exposed 39 cm from roof-mounted antenna (sagittal plane).

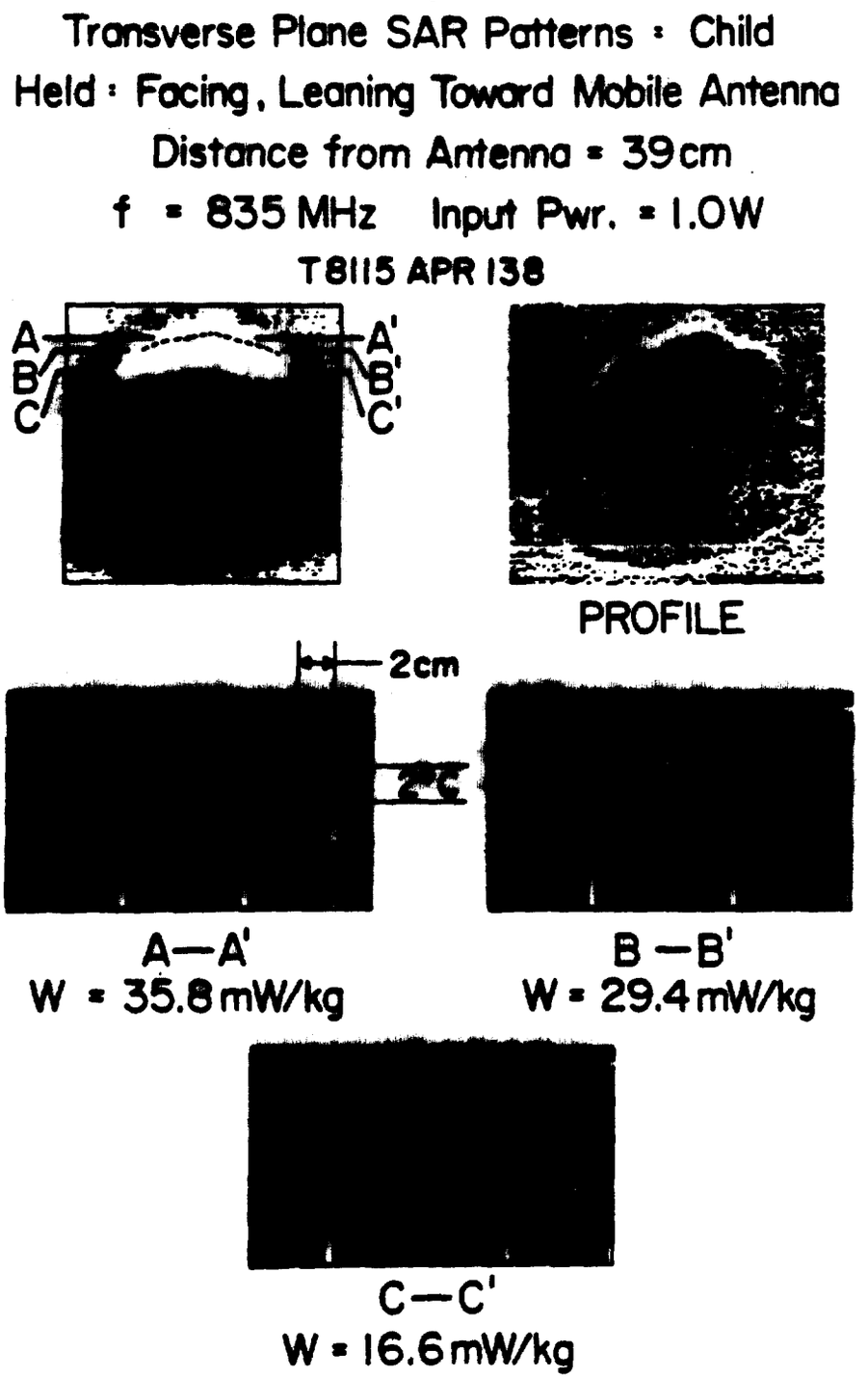

Fig. 52. Thermographically measured SAR patterns in child model exposed 39 cm from roof-mounted antenna (transverse plane through eyes).

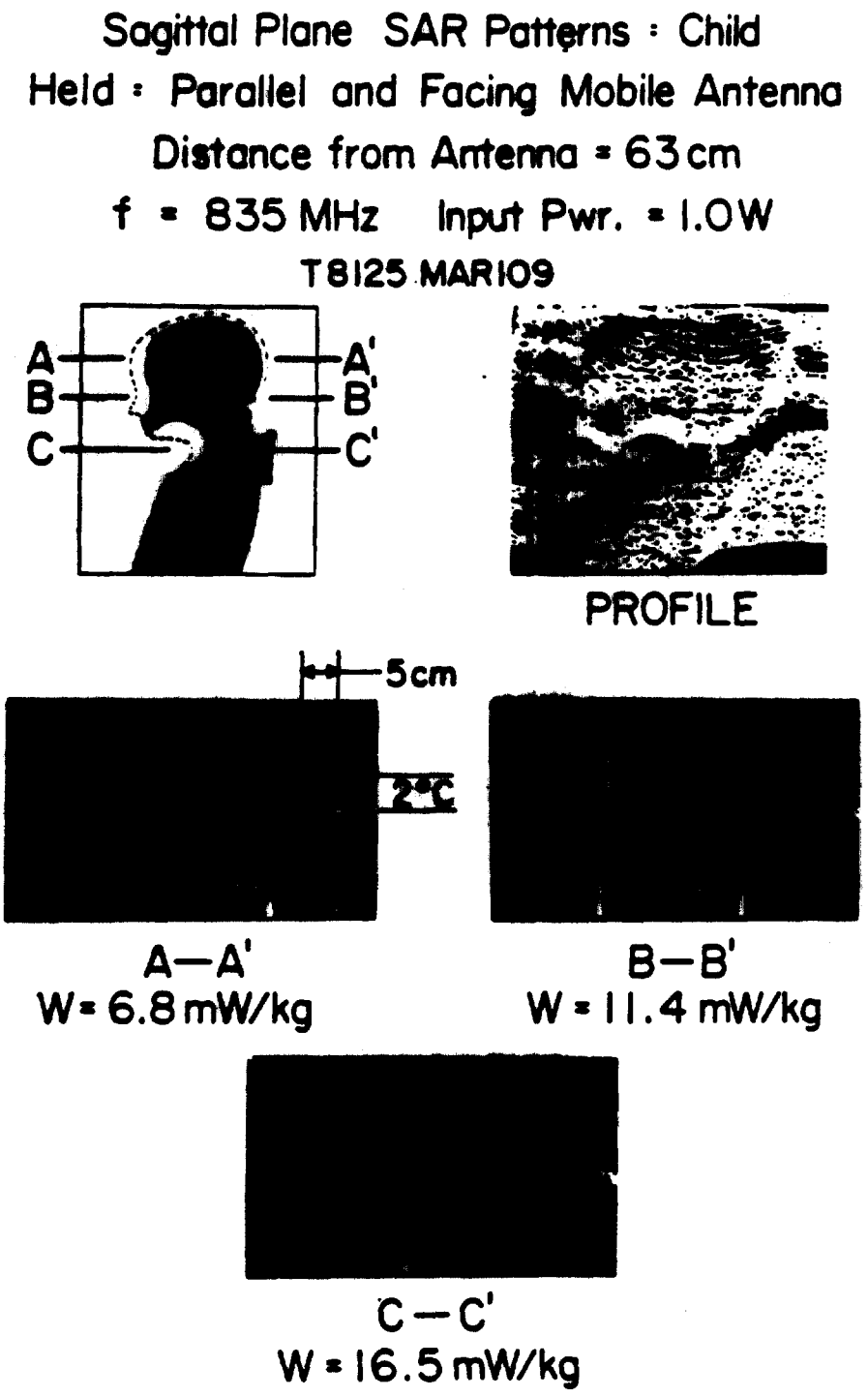

Fig. 53. Thermographically measured SAR patterns in child model exposed 63 cm from roof-mounted antenna (sagittal plane).

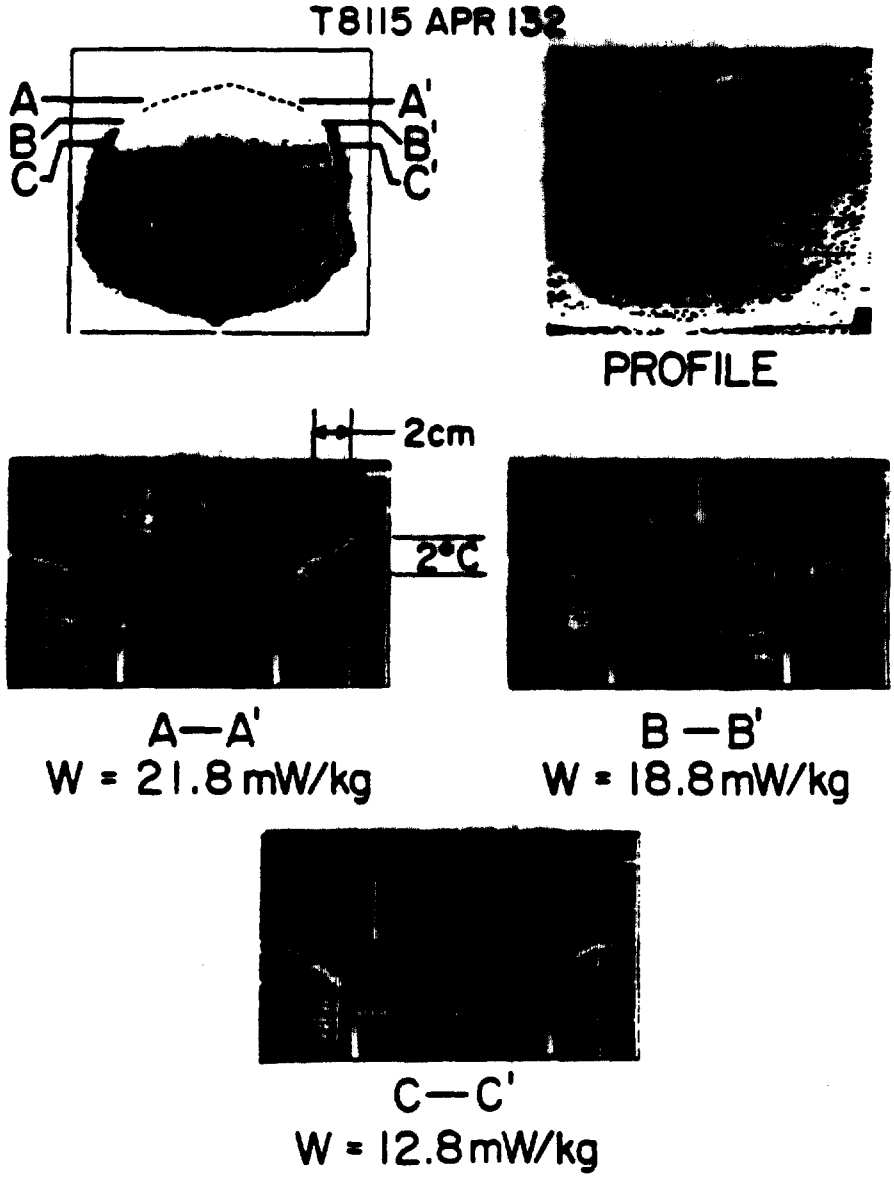

Fig. 54. Thermographically measured SAR patterns in child model exposed 63 cm from roof-mounted antenna (transverse plane).

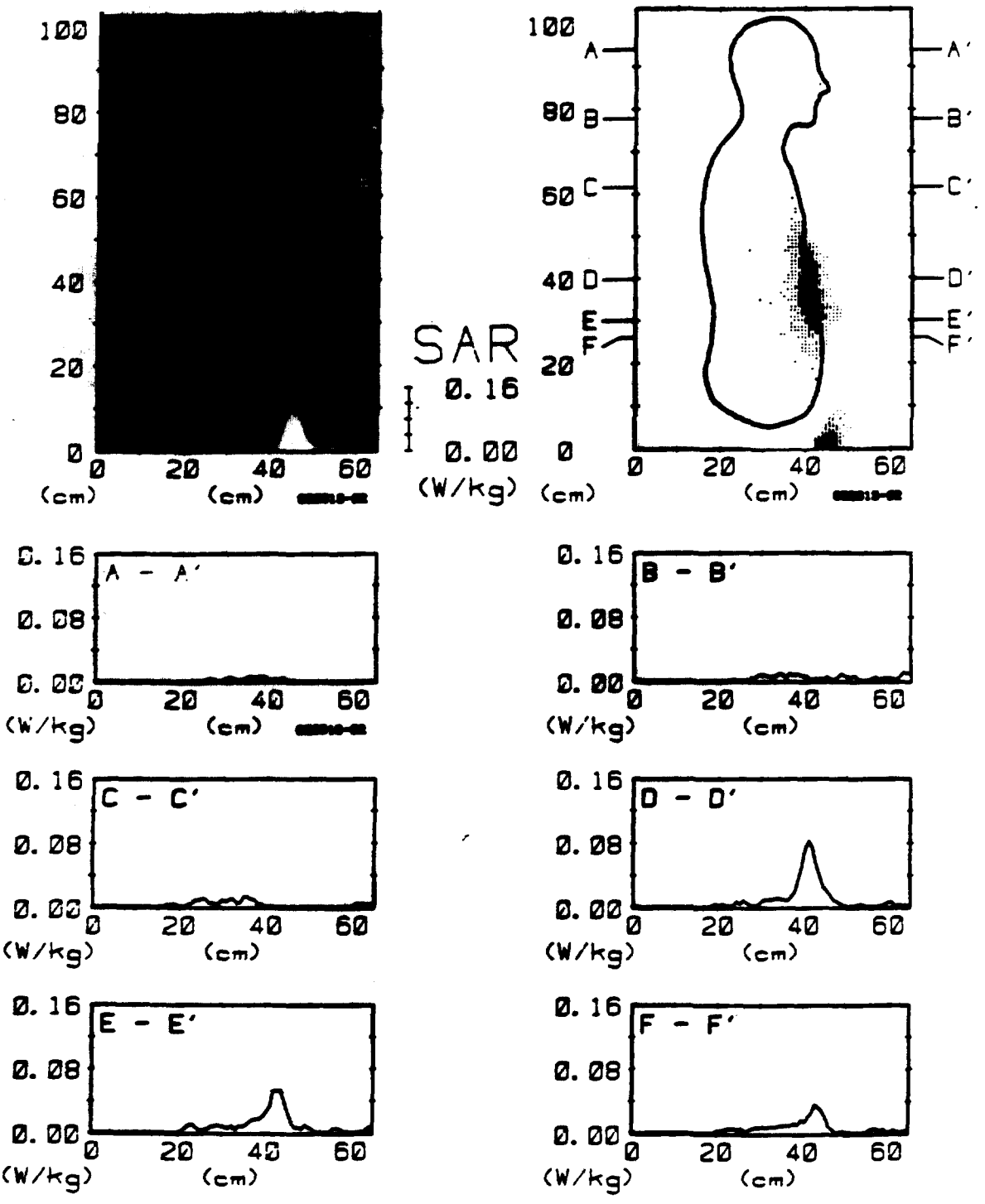

Fig. 55. Computer-processed thermograms showing SAR distribution in sagittal plane of man model exposed to 835-MHz in standing position exterior of automobile 12 cm from trunk-mounted antenna with 1-W input.

We took a closer scan as shown in Fig. 56 to improve the thermograph resolution. With the improved resolution the maximum SAR was found to be .12 W/kg per watt at the surface of the abdomen (D-D's scan). Based on the exposure levels in Fig. 38, it was .28 W/kg per mW/cm^2.

In Figs. 57 and 58 are shown the whole-body and close-up thermograms for the adult-woman model exposed at a distance 9.7 cm from the antenna. The maximum SAR was found to be approximately .20 W/kg per watt input into the antenna, or .32 W/kg per mW/cm^2 exposure level.

Thermograms taken for the foam-clad child model exposed in the standing position 15 cm from the antenna are shown in Figs. 59 and 60. Maximum SAR in the eye region was .23 W/kg per watt input to the antenna, or .64 W/kg per mW/cm^2 incident power density.

Exposure to Fields Inside Car from Trunk-Mounted Antenna

The fiberglass child model was the only model in which SAR distribution from exposure inside of the car was analyzed by thermography. For this series the model was designed to separate in the sagittal plane of the head and neck only, as shown in the photograph in Fig. 28. With the exposure fields identified as shown in Fig. 45, the thermographs shown in Figs. 61 and 62 were obtained. A maximum SAR in the vicinity of the orbital region of the eyes of .012 W/kg per watt input to the antenna or approximately .032 W/kg per mW/cm^2 exposure level was obtained. In Table 6 are illustrated the maximum SAR per watt input to the antenna and maximum SAR per mW/cm^2 that were obtained thermographically for the various exposures from the trunk-mounted antennas.

Vitek 101 Temperature Probe Data

In Tables 7 and 8 are given the SAR data per 1-W input power at various depths of the locations of the heart, kidney, liver, and stomach of

TABLE 6. MAXIMUM SARs IN MODELS EXPOSED TO TRUNK-MOUNTED ANTENNA

	Max. SAR per Watt (W/kg)	Max. SAR per mW/cm^2 (W/kg)
Man outside	0.12	0.28
Woman outside	0.20	0.32
Child outside	0.23	0.64
Child inside	0.01	0.03

TABLE 7. SARs OF STANDING MAN MODEL EXPOSED TO TRUNK-MOUNTED ANTENNA (W/kg PER WATT)

Depth (cm)	Heart	Kidney	Liver	Stomach
1	0.0202	0.0316	0.1020	0.1320
2	0.0128	0.0148	0.0602	0.0832
3	0.0075	0.0081	0.0340	0.0425
4	0.0043	0.0046	0.0188	0.0204
5	0.0023	0.0023	0.0086	0.0089
6	0.0013	0.0013	0.0047	0.0037

TABLE 8. SARs OF STANDING WOMAN MODEL EXPOSED TO TRUNK-MOUNTED ANTENNA (W/kg PER WATT)

Depth (cm)	Heart	Kidney	Liver	Stomach
0.5	0.0207	0.0746	0.117	0.147
1	0.0260	0.0642	0.110	0.135
2	0.0121	0.0307	0.0540	0.0727
3	0.0092	0.0171	0.0289	0.0381
4	0.0042	0.0074	0.0148	0.0189
5	0.0026	0.0034	0.0076	0.0084
6	0.0014	0.0025	0.0039	0.0040

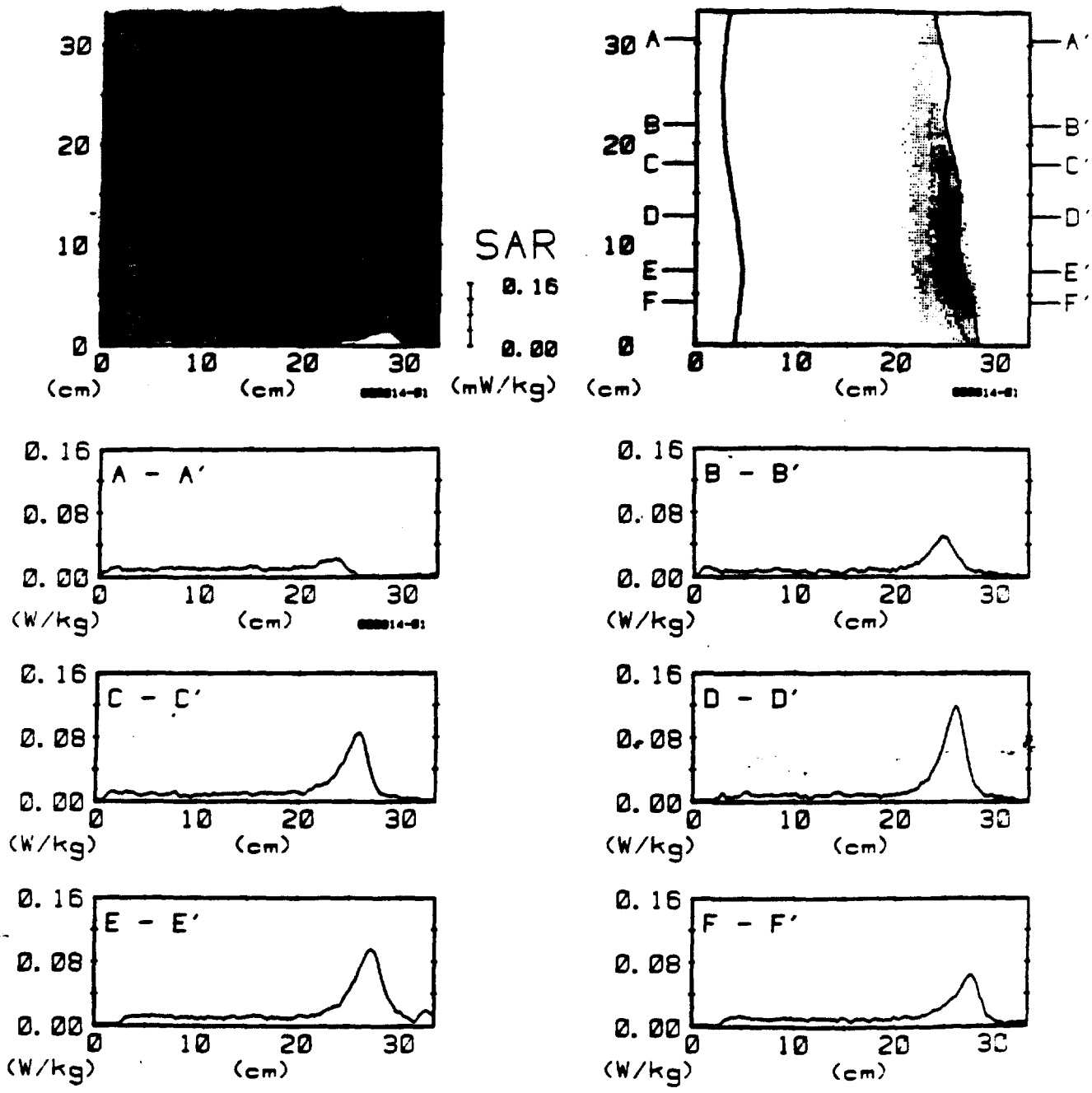

Fig. 56. Closeup thermograms showing SAR distribution in sagittal plane of man model exposed to 835-MHz in standing position exterior of automobile 12 cm from trunk-mounted antenna with 1-W input.